

Satellite and debris characterisation with Adaptive Optics Imaging

M. Copeland, F. Bennet, C. d’Orgeville, V. Korkiakoski, M. Lingham, I. Price and F. Rigaut

Research School of Astronomy and Astrophysics, Australian National University, Canberra, ACT 2611, Australia

Space Environment Research Centre (SERC Limited), Mt Stromlo Observatory, Weston Creek, ACT 2611, Australia

C. Smith

EOS Space Systems Pty Ltd, 55A Monaro Street, Queanbeyan, NSW 2620, Australia

Space Environment Research Centre (SERC Limited), Mt Stromlo Observatory, Weston Creek, ACT 2611, Australia

ABSTRACT

The Research School of Astronomy and Astrophysics (RSAA) at the Australian National University (ANU) has developed the Adaptive Optics Imaging (AOI) system for satellite and debris characterisation in low Earth orbit (LEO) and satellite tracking in geostationary orbit (GEO). We have demonstrated the capability of the system on-sky by performing an AO correction on a star. With AO correction and using lucky imaging to select only the best frames we achieve a strehl ratio of 27%. The effectiveness of the AO correction is evident when comparing open and closed loop images of Cosmos 1656 in LEO. Features such as panels, satellite body and the antenna can be distinguished in the closed loop image that are not visible when using no AO correction. The angular size of features were measured which allowed for physical dimensions of the satellite to be calculated.

1 INTRODUCTION

Atmospheric turbulence is responsible for degradation in performance of ground based telescopes. Convective cells, temperature gradients and wind shear create localised changes in refractive index which distorts the wavefront of light travelling through the medium. The strength of the atmospheric distortion can be measured by a characteristic length r_0 and time scale τ_0 . The system will be limited to a resolution of $\frac{\lambda}{r_0}$ rather than the diameter of the telescope primary mirror [1]. Therefore the performance of the system is dependant on the atmospheric conditions at the time of observation.

Adaptive optics (AO) is a method used to compensate for the wavefront distortions induced by the atmosphere and restore the resolving power on the telescope [2]. An AO system does this by making a real time measurement of the wavefront distortion and applying a correction to return the original condition. An AO system consists of three primary components; a deformable mirror (DM), wavefront sensor (WFS) and control computer which are shown in Fig. 1. Light from the object of interest is collected by the telescope and enters the AO system. The distortion is measured by the wavefront sensor and the control computer processes the measurements and then commands to correct the distortion is sent to the DM. The system operates as a continuous feedback loop to maintain a flat wavefront, which is passed to a camera for the corrected images to be captured.

Send correspondence to M. Copeland (michael.copeland@anu.edu.au)

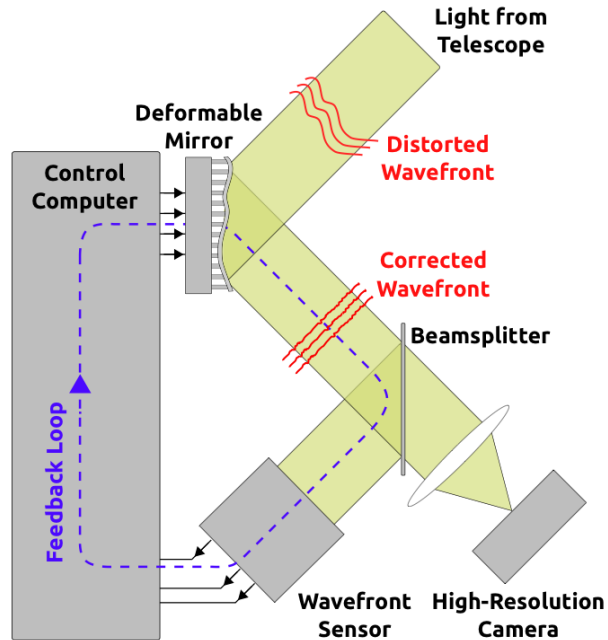


Fig. 1: Schematic of an AO system. The wavefront is measured by the wavefront sensor, and these measurements are translated to correcting commands of the DM by the control computer.

Adaptive optics was first developed for astronomy applications to make capturing higher resolution images of stars, galaxies, and planets possible to improve scientific outcome. However the same principals can be applied for other applications where light passes through a medium which distorts and degrades the signal. Adaptive optics can be used in biomedical imaging, free space communications and in space situational awareness.

Space debris poses an ever increasing threat to a safe and secure space environment, necessitating increased focus on space situational awareness. A single collision with a small piece of debris can cause catastrophic damage to a spacecraft and create further debris which can then collide with other objects. If the density of debris becomes large there is a chance of a Kessler Syndrome occurring in which a single collision creates a cascade of debris making it impossible for spacecraft to occupy certain orbits [3].

Optical measurements are used for accurate tracking and characterisation of objects. Active tracking through satellite laser ranging (SLR) and debris laser ranging offer the most precise form of tracking, while passive tracking is also possible with through direct imaging [4, 5]. The position is measured by finding the centroid in an image of a sunlit object in conjunction of telescope pointing. These measurements will be impacted by atmospheric effects causing the image to become distorted and jitter which can reduce accuracy in centroid measurements. Thus adaptive optics are needed to correct for the atmospheric effects which will eliminate the jitter and improve the resolution to allow a more accurate centroid to be measured.

The size and shape of an object will affect how some external forces act upon them. Atmospheric drag, solar radiation pressure and gravitational forces are some such variables [6]. Knowledge of object characteristics are required for accurate orbit predictions. Objects cannot be constantly tracked and therefore a prediction must be made so the position is known and any possible collisions will be identified. Characteristics are typically approximated as no information of the object may be known which reduces accuracy in the orbital models [7]. Inaccuracy in orbital models will mean that collision predictions may not have high confidence and less warning time to take mitigating action. Higher accuracy in collision predictions necessary to maintain safe utilisation of the space environment.

2 SYSTEM OVERVIEW

The Adaptive Optics Imaging (AOI) system has been developed for object characterisation and tracking through high resolution imaging by the Research School of Astronomy and Astrophysics (RSAA) at the Australian National University (ANU). AOI operates on the EOS Space Research Centre 1.8 m telescope located in Canberra, Australia. With AOI we will have a resolution of 50 cm for objects at 800 km range and 800 nm imaging wavelength to perform size, shape and orientation characterisation on low Earth orbit (LEO) objects. Positional measurements for satellites in geostationary orbit (GEO) can be made by measuring position relative to the known location of a reference star [8].

AOI has an imaging field of view of 22 arcseconds across a 512×512 pixel EMCCD camera. We operate the camera at between 30 and 60 Hz for lucky imaging and to freeze out tip-tilt and field rotation. Lucky imaging allows for only the best frames to be selected where the atmospheric turbulence is low and the correction applied by the AO system is best.

3 ON-SKY VERIFICATION

Initial on-sky observations with AOI were conducted with stellar sources. Fig. 2 is 100×100 pixel crop of a single frame captured of a star while the system was running in open loop. In open loop there is no AO correction being applied so the effect of atmospheric distortion are evident. An ideal image of a point source with AOI should be 4 pixels in size, however the image observed is greater than 20 pixels in size. This is due to the effects of the atmospheric turbulence limiting the effective resolution of the system and causing speckle. The star image is also continually jumping on the detector making it difficult to pinpoint the position which would lead to inaccurate positional measurement.

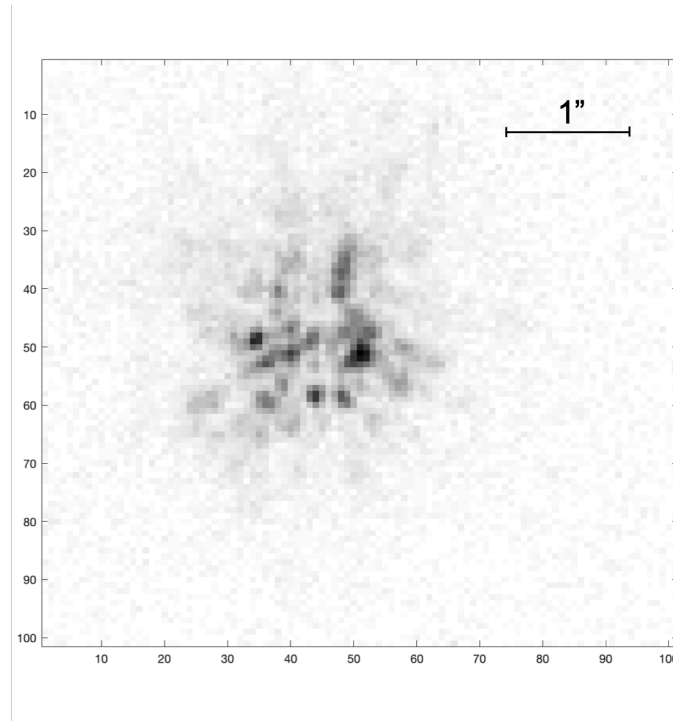


Fig. 2: Open loop image of star captured with AOI

We make use of image stacking to improve the signal to noise and image quality. Fig. 3 (a) shows all open loop frames stacked together and averaged. By averaging all the frames we observe the effect of the jitter induced by the atmosphere and the resulting average spot is very large and spread over many pixels. To improve this image, we use a simple shifting and stacking method by aligning all frames based on the peak pixel and computing the average of all

those frames. The image is further improved by using lucky imaging and selecting only the best frames. Fig. 3 (b) is the stacked image of the top 5% frames based on the peak value. We employ lucky imaging by selecting only the frames with the highest peak values. In these frames the atmospheric distortion is lessened and the star light is more likely to be concentrated in a smaller core. From the shifted and stacked image in Fig. 3 (b) we measure the full width half maximum (FWHM) to determine the spot size of 6.3 pixels.

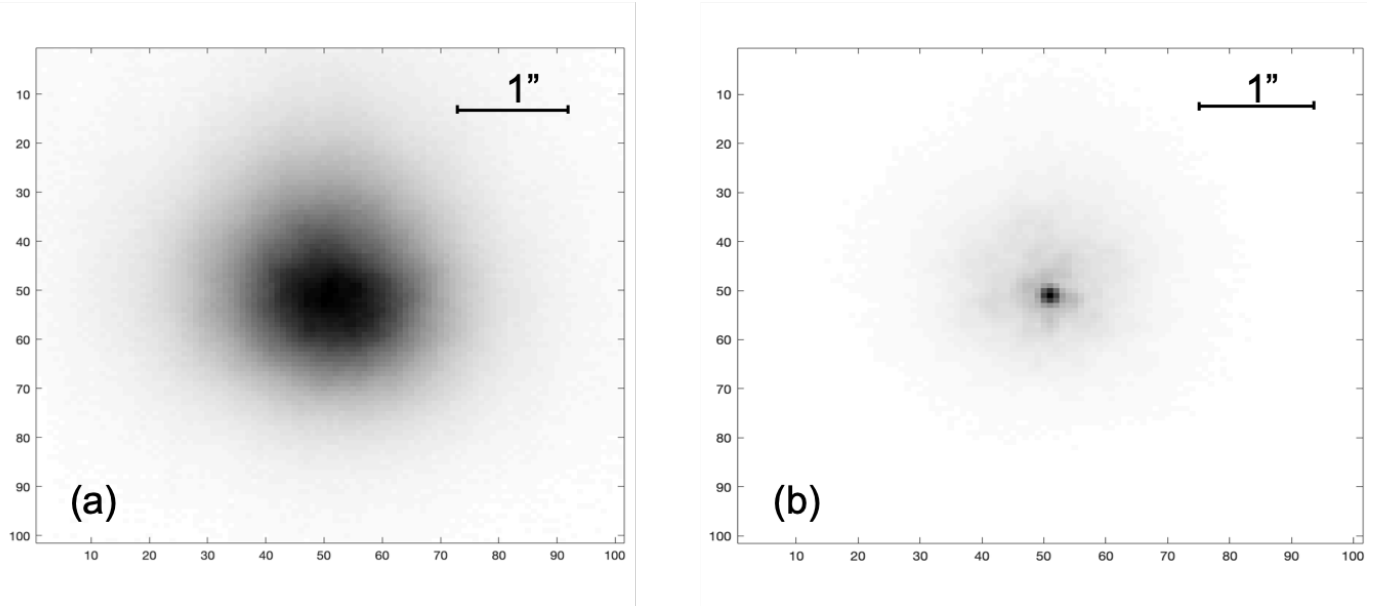


Fig. 3: (a) All images captured stacked and averaged with no shifting. Right: Top 5% of images shifted based on the peak pixel position, then stacked and averaged

Closing the AO loop improves the image with the spot size becoming smaller and peak intensity increasing. As with the open loop images we use lucky imaging to select only the with the top 5% peak pixel values of all captured images. The selected images are shifted and stacked together to improve signal to noise in a processed image. Fig. 4 shows the closed loop image of the same star as shown in Fig. 2 while the system was running in open loop. The peak intensity in the image is increased by a factor of 4 over the best stacked open loop image. The energy in the closed loop image is much more concentrated giving a higher peak value and smaller spot size. The FWHM of the spot is measured as 3.5 pixels which shows that the energy is more concentrated in the closed loop image compared to the open loop case where the FWHM was 6.3 pixels. This is shown in Fig. 5 where the cross sectional profiles of the stacked open loop and closed loop images are plotted.

The Strehl ratio provides us with a measure of the performance of the system relative to an ideal case. We applied a Gaussian fit to the peak of the closed loop image and compared that to an ideal psf based on the specifications of the system. The peak value of the ideal psf is determined by making the integral of the psf equal to the integral of the capture frame, which ensures the energy in the ideal spot is equal to that of the measured one. The Strehl ratio is then given by Eq. 1.

$$Strehl = \frac{peak\ of\ measured\ spot}{peak\ of\ ideal\ psf} \quad (1)$$

We calculate a Strehl ratio of 27% for the closed loop image. The design specification for AOI was a Strehl ratio of 30%, therefore some improvement can be made to improve the performance of the system but it is operating near the design specification. The stacked open loop image has a Strehl ratio of 7% which shows that the AO correction produces a significant improvement over open loop with lucky imaging.

Images of a binary star system were captured to determine the plate scale of AOI. Fig. 6 shows a closed loop image of a binary system with separation of 0.5 arcseconds. We measure the separation of the stars in the image to be 10.1

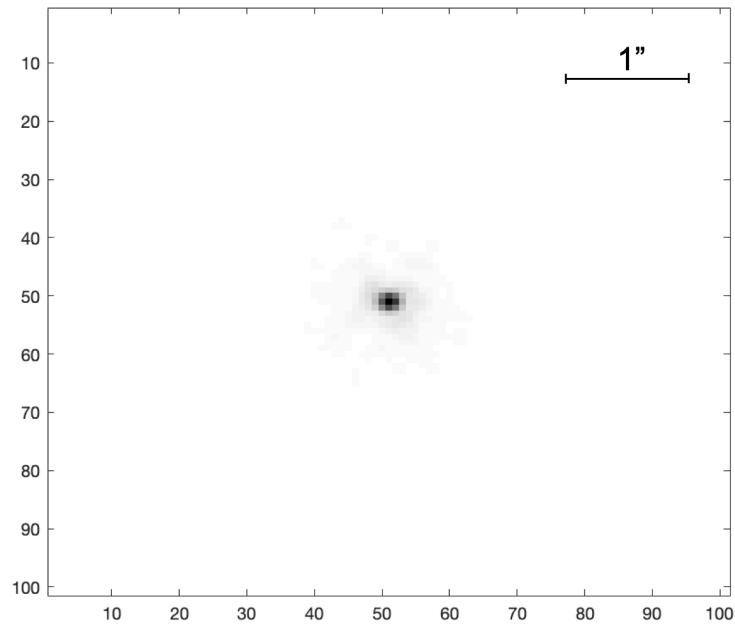


Fig. 4: Closed loop image of star captured with AOI

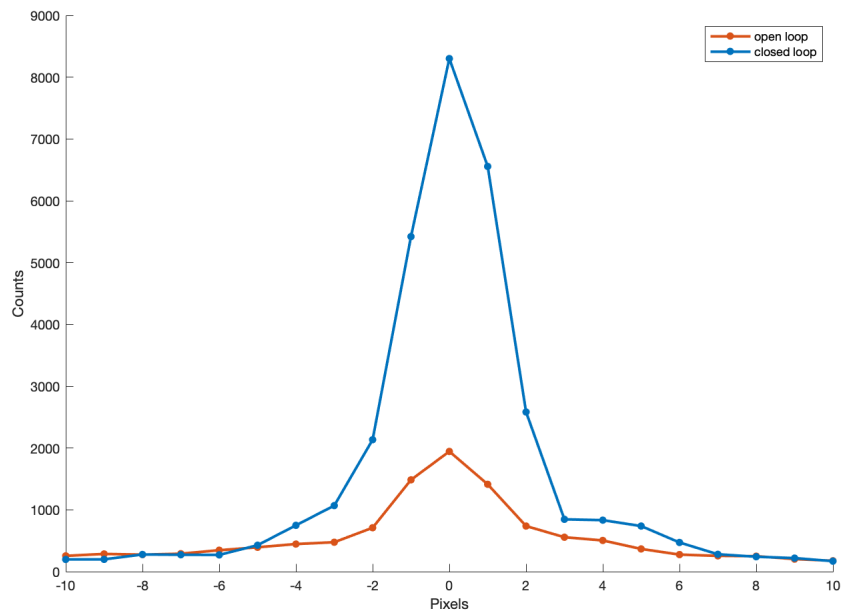


Fig. 5: Comparison of cross-sectional profile between stacked open loop image and closed loop image

pixels, thus the plate scale of the system is 0.049 arcseconds/pixel. The imaging camera detector size of 512×512 pixels gives a total field of view of 25 arcseconds.

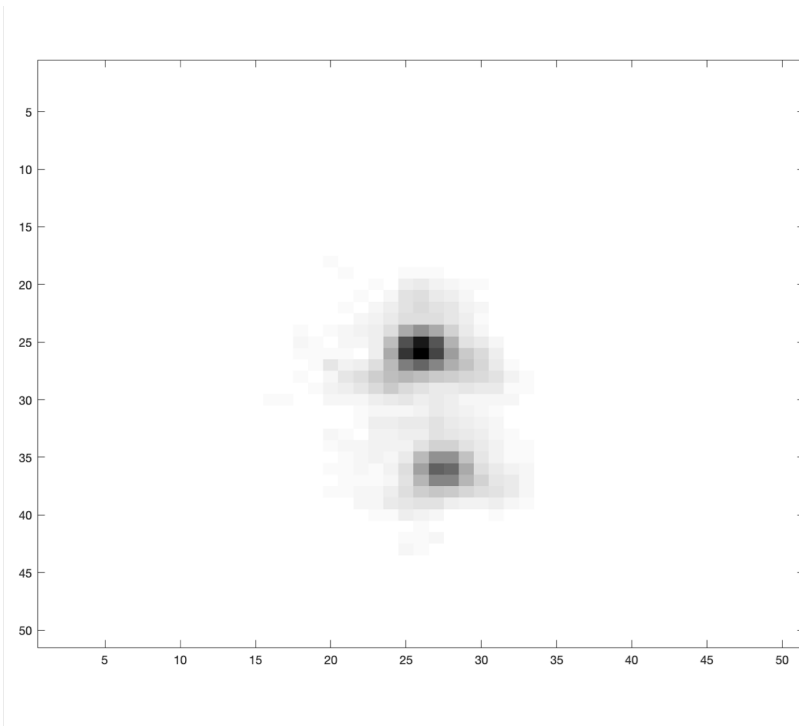


Fig. 6: Closed loop image of binary star system with 0.5 arcsecond separation

4 LEO OBJECT IMAGING

Following verification of the AO performance on stellar sources AOI was used to image LEO targets. Objects were selected based on predicted brightness, maximum elevation, and orbit altitude. Objects with a peak elevation of greater than 70 degrees were preferred so the telescope is looking through less atmosphere for improved imaging performance. Similarly we chose objects with orbits of between 750 and 1000 km, which allowed the system sufficient resolution to distinguish features and not cause the telescope to slew quickly across the sky which degrades the performance of the system.

The first successful closed loop results were obtained with Envisat. The captured images were stacked together using cross correlation to determine where a single image best fits over the stack. Fig 7 shows the stacked image of Envisat. We use a cross correlation stacking technique as registration of the images is more accurate on an extended object.

There are two separate features in the image which likely correspond to the body of the satellite and solar panel array which is extended out the front. The overall shape of the body or solar panel array can not be determined from the image, however the atmospheric conditions were poor during the observations and the distortions introduced by the atmosphere were likely larger than the AO system is able to correct effectively.

Observations during good atmospheric conditions yielded improved imaging performance. Fig. 8 shows a stacked image of Cosmos 1656 while running in closed loop at a rate of 1 kHz. In this image several features can be distinguished, such as solar panels or communications array extending from the main body of the satellite. There is also a thin antenna extending out from the top of the main body.

At the time of capture the satellite was at a range of approximately 1050 km. Given the known plate scale of 0.049 arcseconds/pixel measured from the binary star system we make measurements of the satellite features to determine angular size. Based on the range estimation a physical size can be made with the angular and physical size shown in Table 1.

Images of Cosmos 1656 were also capture in open loop. Fig. 9 shows a stack of open loop images. To create the stack

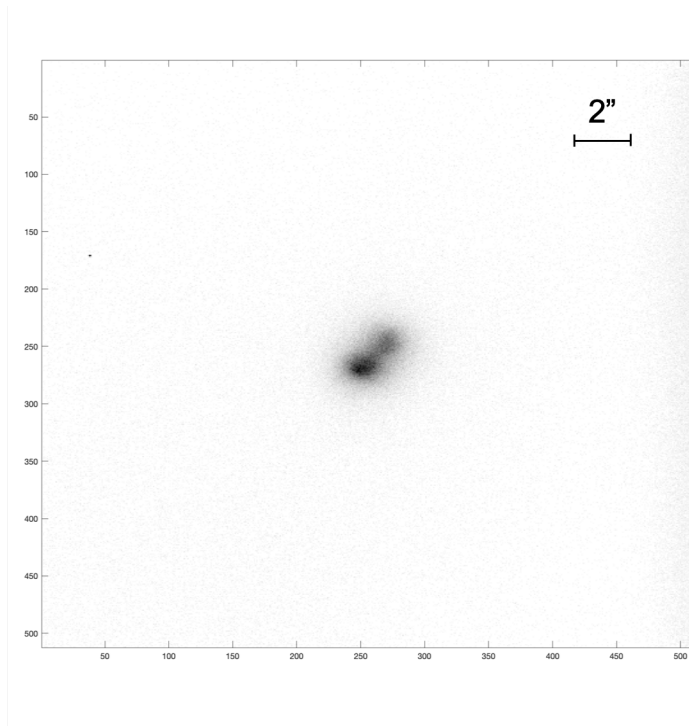


Fig. 7: Closed loop image of Envisat stacked with cross correlation lucky imaging

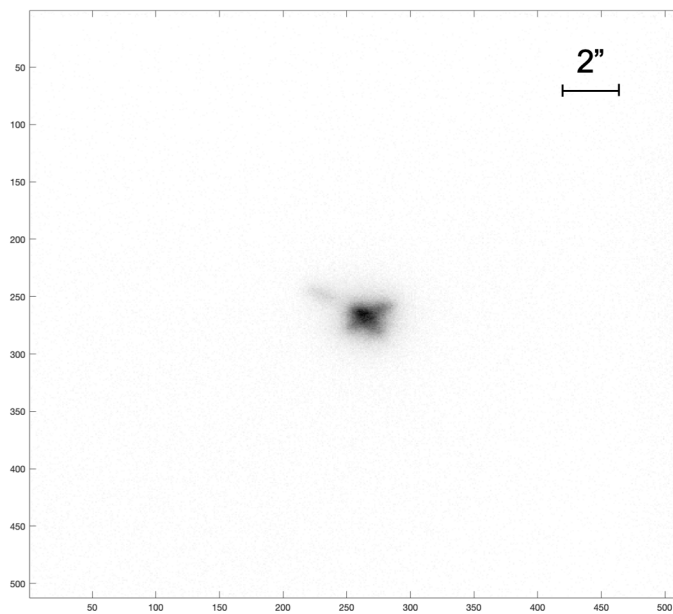


Fig. 8: Closed loop image of Cosmos 1656 stacked with cross correlation lucky imaging

we chose the top 10% of frames based on the peak value and used cross correlation to stack them together. In the open loop images the features that were seen in Fig ref are not evident. The peak intensity is reduced to approximately half,

Table 1: Size measurements of Cosmos 1656 features

Description	Angular size (arcseconds)	Physical size (m)
Lower panel array span	2.2	10.8
Body width	0.59	2.9
Antenna length	1.6	8.0
Body length	1.7	8.4

due to the light being distributed over a larger area on the detector. Therefore the AO system has made a significant improvement in the imaging quality of the system.

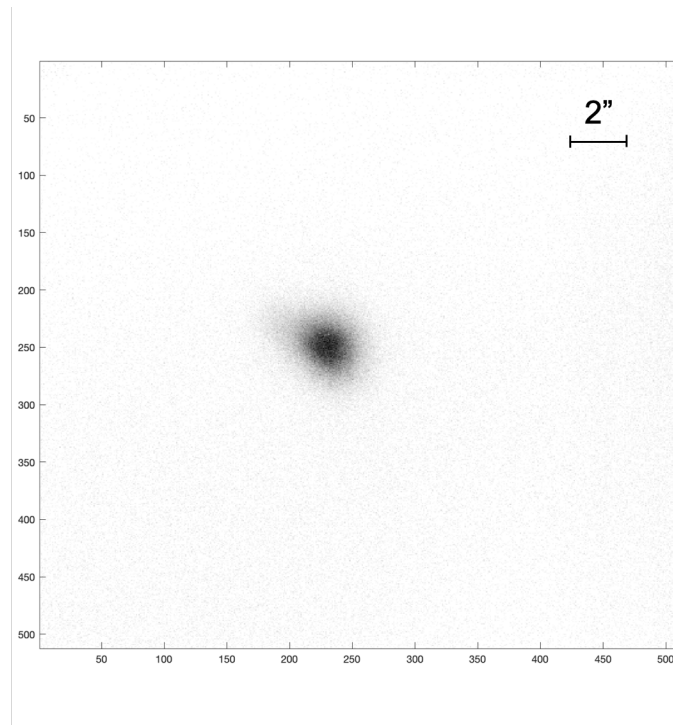


Fig. 9: Open loop image of Cosmos 1656 stacked with cross correlation lucky imaging

5 CONCLUSION

We have demonstrated the effectiveness of the adaptive optics correction on stellar and LEO objects. We compared open and closed loop images of a star and found a significant improvement when using the AO correction. The closed loop image of a star gave us a Strehl ratio of 27%, which is close to the design specification of 30%. Closed loop images of Evisat yielded two distinct features, the satellite body and solar array. We demonstrated a improvement of image quality with AO correction on Cosmos 1656. With AO several features becoming apparent that were not visible in open loop. We measured the angular size of the features identified and based on range at the time of image capture we estimated the physical dimensions of the satellite features.

6 ACKNOWLEDGEMENT

The authors would like to acknowledge the support of the Cooperative Research Centre for Space Environment Management (SERC Limited) through the Australian Governments Cooperative Research Centre Programme.

This research is supported by an Australian Government Research Training Program (RTP) Scholarship.

REFERENCES

- [1] D. L. Fried, “Anisoplanatism in adaptive optics,” *Journal of the Optical Society of America*, vol. 72, no. 1, p. 52, 2008.
- [2] J. M. Beckers, “Adaptive optics for astronomy: Principles, Performance and Applications,” *Annu. Rev. Astron. Astrophys.*, vol. 31, pp. 13–62, 1993.
- [3] D. J. Kessler and B. G. Cour-Palais, “Collision frequency of artificial satellites: The creation of a debris belt,” *Journal of Geophysical Research*, vol. 83, no. A6, p. 2637, 1978.
- [4] J. Degnan, “Satellite Laser Ranging: Current Status and Future Prospects,” *IEEE Transactions on Geoscience and Remote Sensing*, vol. GE-23, no. 4, pp. 398–413, 1985.
- [5] G. Kirchner, F. Koidl, F. Friederich, I. Buske, U. Völker, and W. Riede, “Laser measurements to space debris from Graz SLR station,” *Advances in Space Research*, vol. 51, pp. 21–24, 2013.
- [6] C. Fruh, M. Jah, and T. Kelecy, “Coupled Orbit-Attitude Dynamics of High Area-to-Mass Ratio (HAMR) Objects: Influence of Solar Radiation Pressure, Earth’s Shadow and the Visibility in Light Curves,” *Celestial Mechanics and Dynamical Astronomy*, vol. 117, no. 4, pp. 385–404, 2013.
- [7] M. Lachut and J. Bennett, “Towards Relaxing the Spherical Solar Radiation Pressure Model for Accurate Orbit Predictions,” in *Advanced Maui Optical and Space Surveillance Technologies (AMOS) Conference*, 2016.
- [8] M. Copeland, F. Bennet, A. Zovaro, F. Riguat, P. Piatrou, and V. Korkiakoski, “Adaptive Optics for Satellite and Debris Imaging in LEO and GEO,” *Advanced Maui Optical and Space Surveillance Technologies (AMOS) Conference*, 2016.